

Non-local diffusion and the chemical structure of molecular clouds

J. J. Martinell,^{1*} D. del-Castillo-Negrete,² A. C. Raga¹ and D. A. Williams³

¹*Instituto de Ciencias Nucleares, Universidad Nacional Autónoma de México, Ap.P. 70–543, 04510 D.F., México*

²*Oak Ridge National Laboratory, Oak Ridge, TN 37831-6169, USA*

³*University College, Gower St., London*

Accepted 2006 July 19. Received 2006 June 28; in original form 2006 April 5

ABSTRACT

We present an application of a non-local turbulent transport model (currently being used to model transport in magnetically confined laboratory plasmas) to the study of the chemical structure of a molecular cloud. We consider a ‘toy model’ chemistry with a single molecular species which is adsorbed/desorbed from grain surfaces. With this idealized chemistry, we are able to find analytic solutions to both the ‘classical’ turbulent diffusion model as well as to the non-local transport model. For the turbulent diffusion model, we find that for the turbulent transport to be important one needs a mixing length comparable to the size of the cloud. On the other hand, with the non-local transport model we find that the chemistry is already strongly affected by the turbulent transport for mixing lengths two orders of magnitude smaller than the cloud size. This model then has the desirable property of being able to mix material over long distances (compared with the size of a molecular cloud) without requiring an inordinately large characteristic size for the turbulent eddies.

Key words: ISM: kinematics and dynamics.

1 INTRODUCTION

In high-density regions of interstellar molecular clouds, atoms and molecules in the gas freeze out on to the surfaces of dust grains. This happens on a relatively short time-scale, $\sim 10^9/n$ years, where n is the total hydrogen nucleon number density (Iglesias 1977; Rawlings et al. 1992). The molecular ices thus formed are readily detected spectroscopically through absorption in pure vibrational lines of the molecules contained within them (e.g. Whittet 2002), and are mainly H₂O (formed by surface hydrogenation of incident O atoms), CO (formed in the gas phase and frozen out), CO₂ (formed by chemical processing of the ices), along with other minor species. The radial dependence of ice abundance across dense cores can now be mapped (Redman et al. 2002) and is shown to increase towards the centre. The amount of ice requires at least one freefall time to be deposited.

Although freeze-out is evidently an efficient process, atoms and molecules are observed to be widely distributed throughout molecular clouds, and mechanisms by which ices are returned to the gas are necessary (Williams & Hartquist 1984). Local non-thermal processes such as heating of grains by the passage of cosmic rays (Leger, Jura & Omont 1985) or by surface reactions (Willacy & Williams 1993) may play a role but are dominated by freeze-out. An idea whose chemical consequences have been widely explored is that a fluid parcel of gas from the interior of a cloud may through

turbulence driven by stellar winds (Norman & Silk 1980) be transported to other regions to experience shocks or other means of desorption (Boland & de Jong 1982; Williams & Hartquist 1984; Charnley et al. 1988a,b; Chièze & Pineau des Forêts 1989; Chièze, Pineau des Forêts & Herbst 1991; Nejad et al. 1990). Charnley et al. (1988b) showed that chemical limit cycles could persist in such periodic cycling of cloud material. On the basis of observational studies by Morata, Girart & Estalella (2003, 2005), Garrod et al. (2005) and Garrod, Williams & Rawlings (2006) have developed a model in which molecular clouds are considered as ensembles of transient cores that grow from a low-density background and decay on a time-scale of approximately one million years. This model has similarities to other cyclic models though the trajectories are simpler than those of, e.g. Charnley et al. The Garrod et al. (2006) models produce simulated molecular intensity contour plots that have closely similar morphologies to those observed.

Xie, Allen & Langer (1995) developed a very different approach based on turbulent diffusion. In turbulent diffusion models, one models the transport due to the turbulent motions in terms of an ‘eddy diffusivity’ $D = \lambda c_s$, where c_s is the sound speed and λ is the eddy size or mixing length. Xie et al. (1995) concluded that in order to have a turbulent transport that has an important effect on the chemical structure of a molecular cloud, one needs $\lambda \sim L$, where L is the characteristic size of the cloud. On the other hand, applying mixing length turbulence models to laboratory experiments one finds that $\lambda \sim 0.01L$ (with L being the characteristic size of the flow), see, e.g. Cantó & Raga (1991). This discrepancy between the mixing length values required by Xie et al. (1995) and the ones

*E-mail: martinell@nucleares.unam.mx

determined from laboratory experiments is an important problem in the application of turbulent diffusion models to the chemistry of molecular clouds. Diffusive models are therefore generally applied to narrow interfaces between media such as hot tenuous winds and cold dense clouds (see Rawlings & Hartquist 1997, and references therein). Chemical tracers of the interfaces in which turbulent diffusion occurs can be identified, and may account for chemical anomalies (e.g. Viti, Natarajan & Williams 2002), but the interfaces are very thin.

In this paper, we present an application of a different turbulent transport model to the problem of the chemistry of molecular clouds. The proposed models are based on the use of a class of integro-differential operators known as fractional derivatives. del-Castillo-Negrete, Carreras & Lynch (2003) introduced the use of these operators to model non-local transport in non-linear reaction-diffusion systems in which the chemistry is described in terms of a simple autocatalytic reaction. More recently, del-Castillo-Negrete, Carreras & Lynch (2004, 2005) used these fractional operators to model anomalous turbulent transport in magnetically confined plasmas. These transport models include non-local effects (i.e. the communication between spatially disconnected regions of the flow), which can simulate the effects of ‘avalanches’ or ‘clumps’ in plasma turbulence. In a molecular cloud, the non-local nature could be due to the effects of ‘jets’ which travel considerable distances within the cloud.

In order to illustrate the properties of this transport model we apply it to a situation deep inside a molecular cloud where the chemistry is dominated by freeze-out and desorption, i.e. where the time-scales for freeze-out (and desorption, if competitive) are shorter than gas-phase chemical time-scales. Therefore, in this simple approximation we can ignore the many rate equations for the individual chemical reactions and focus on interactions with the grain surfaces. With this limitation, we are able to obtain full analytic solutions which show the interesting properties of the non-local transport model. A comment on this approximation is in order. It is well known that the chemical time-scale and the freeze-out time-scale are comparable in interstellar gas of a density around 10^4 total hydrogen per cm^3 with canonical parameters (e.g. Williams 2003). But the main gas-phase chemical reactions affecting CO in molecular clouds ensure that CO maintains a near uniform abundance relative to hydrogen (the observations tend to show that CO/H₂ is fairly constant at about 10^{-4}). Freeze-out to dust grains therefore becomes an important loss mechanism, as is frequently observed (e.g. Redman et al. 2002). Thus, to a first approximation, we are justified in considering the diffusion model in terms of its influence on freeze-out.

This paper is organized as follows. In Section 2, we discuss the adsorption/desorption model for the cloud chemistry, and use it in a standard, turbulent diffusion transport model. We then study the properties of the adsorption/desorption model in terms of the non-local transport operators introduced in del-Castillo-Negrete et al. (2003). Section 3 is devoted to the study of weak non-locality, and Section 4 addresses the more general problem of transport in clouds in the presence of strong non-locality. Finally, in Section 5 we present a summary of our results.

2 ADSORPTION AND DESORPTION WITHIN A MOLECULAR CLOUD

Let us consider the fraction f of molecules of a representative chemical species (which we will take to correspond to CO, the most important *molecule* that freezes out in cloud interiors) which is present

in the gas phase (a fraction $1 - f$ of the molecules would then be adsorbed on to grain surfaces). The adsorption rate for this species is given by

$$R = f n_g q, \quad (1)$$

with

$$q = S \sigma_g c_0, \quad (2)$$

where c_0 is the mean thermal velocity of CO, n_g is the number density of grains, S is the sticking coefficient and $\sigma_g = \pi r_g^2$ is the geometrical cross-section of the grains. We now assume that we have $S = 1$ and $r_g = 10^{-5}$ cm. If we consider the empirically determined extinction of 1.6 mag per kpc, the number density of grains (with our assumed $r_g = 10^{-5}$ cm radius) is $n_g \approx 10^{-12} n$ (where n is the number density of H nuclei). With these values, from equations (1) and (2) we obtain (in terms of the sound speed c_s),

$$R = \frac{f c_s}{d}, \quad (3)$$

with

$$d \equiv \left(\frac{10^5 \text{ cm}^{-3}}{n} \right) (10^{17} \text{ cm}), \quad (4)$$

being a characteristic length associated with the adsorption process. In equation (4), we have introduced a typical number density (of H nuclei) of 10^5 cm^{-3} for a dense molecular cloud (Steinacker et al. 2005), and considered that the ratio between the sound speed c_s and the CO thermal velocity is $c_s/c_0 = \sqrt{7\gamma} = 3.13$ (with $\gamma = 1.4$ being the specific heat ratio).

We have also to consider the desorption rate. We assume that there is a region of the cloud in which CO is fully desorbed; in the Taurus Molecular Cloud, this is a region up to approximately five visual magnitudes from the cloud edge (Whittet 2002). We set the origin of our spatial coordinate system and $f = 1$ at this position, and consider only the adsorption process (with the rate given by equations 3 and 4) in the interior of the cloud.

If we assume a slab geometry for the cloud, the steady, turbulent diffusion transport problem (see e.g. Xie et al. 1995) then reduces to solving the equation

$$D \frac{d^2 f}{dx^2} = R, \quad (5)$$

where x is the depth into the cloud. In this equation, R is the adsorption rate coefficient (given by equation 3) and

$$D \equiv \lambda c_s \quad (6)$$

is the turbulent diffusion coefficient defined in terms of the mixing length λ and the thermal velocity c_s . Combining equations (3), (5) and (6), one obtains the equation

$$\frac{d^2 f}{dx^2} = \frac{f}{\lambda d}, \quad (7)$$

which for constant d (i.e. for a cloud of constant density), and with the boundary conditions $f(0) = 1$ and $f(x) \rightarrow 0$ for $x \rightarrow \infty$ can be directly integrated to obtain

$$f(x) = e^{-x/l}, \quad \text{with } l = \sqrt{\lambda d}. \quad (8)$$

From equation (8), we see that the fraction f of molecules (of the chosen, representative species) present in the gas phase decreases exponentially into the cloud, with an e -folding length $l \propto \lambda^{1/2}$ (where λ is the mixing length of the turbulent diffusion model). In Fig. 1, we show l as a function of λ for a $n = 10^5 \text{ cm}^{-3}$ mean cloud density (solid line).

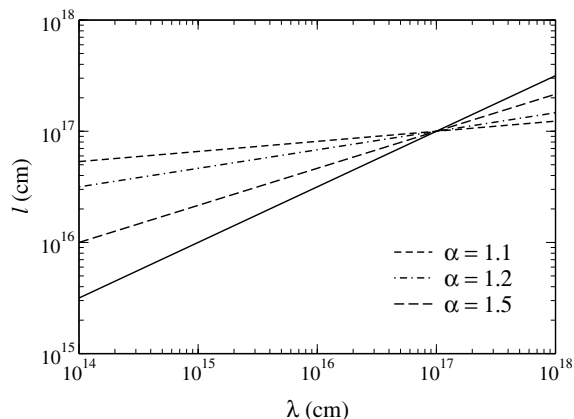


Figure 1. Penetration length as a function of the mixing length for the standard diffusion model (solid line) and for three values of the fractional parameter α .

In order to better understand the implications of this figure, we consider for example a molecular cloud core with a size of 0.1 pc. We assume that the region where desorption is negligible is about half the core size, which in turn is half the distance to the centre, so that the characteristic length is $L \sim 0.2(0.1 \text{ pc}) \sim 6 \times 10^{16} \text{ cm}$. The cloud density is $n = 10^5 \text{ cm}^{-3}$ (Steinacker et al. 2005). If we have $\lambda = 0.01L \sim 6 \times 10^{14} \text{ cm}$, we obtain an e -folding length $l \sim 7 \times 10^{15} \text{ cm}$. The effect of the turbulent diffusion is therefore only seen in the outer 10 per cent or so of the size of the cloud.

If we want the turbulent diffusion to affect all the relevant volume in the cloud, we need to have $l \sim L \sim 6 \times 10^{16} \text{ cm}$. From Fig. 1, we see that this value is reached only for $\lambda \sim 4 \times 10^{16} \sim L$ (in other words, for a mixing length comparable to the characteristic size of the cloud). In this way, with our simple analytic model, we re-obtain the qualitative behaviour of the numerical results of Xie et al. (1995).

3 NON-LOCAL TURBULENT TRANSPORT MODEL

Standard diffusive transport is associated with an underlying ‘microscopic’ Brownian random walk in which particles exhibit uncorrelated, Gaussian-distributed jumps. In this case, transport is local, and the particle distribution function is described by an equation involving second-order derivatives in space of the type of equation (5). However, if the probability distribution function of jumps is non-Gaussian (in particular, if it has divergent second-order moments) the particles exhibit anomalously large displacements known as Levy flights, transport is non-local, and the particle distribution is governed by a fractional diffusion equation (see e.g. Metzler & Klafter 2000, and references therein). For the steady-state situation we are considering, the equation for f takes the form,

$$D_\alpha \frac{d^\alpha f}{dx^\alpha} = R, \quad (9)$$

where $1 < \alpha < 2$. Reaction-diffusion equations of this type have been studied by del-Castillo-Negrete et al. (2003), for the time-evolution of shock fronts. For our case, we are only interested in the final steady state. The turbulent fractional diffusion coefficient now is given by

$$D_\alpha \equiv \lambda^{\alpha-1} c_s. \quad (10)$$

Combining equations (3), (9) and (10), one obtains the equation

$$\frac{d^\alpha f}{dx^\alpha} = \frac{f}{\lambda^{\alpha-1} d}. \quad (11)$$

There are different ways of defining a fractional derivative, depending on the integration limits of the integral involved. These derivatives constitute a generalization of standard calculus which has been used recently in many problems of applied sciences (for technical aspects of fractional derivatives see Podlubny 1999). We first solve equation (11) in a simple way that illustrates the effect of non-local transport. For this, we use for the fractional derivative, the right-fractional Riemann–Liouville definition of order α ($1 < \alpha < 2$), namely, $d^\alpha f/dx^\alpha = {}_x D_\infty^\alpha f$, with

$${}_x D_\infty^\alpha f = \frac{1}{\Gamma(2-\alpha)} \frac{d^2}{dx^2} \int_x^\infty \frac{f(t) dt}{(t-x)^{\alpha-1}}. \quad (12)$$

Using the fact that ${}_x D_\infty^\alpha e^{-\mu x} = (\mu)^\alpha e^{-\mu x}$, for $\mu > 0$, we get the solution of equation (11) with boundary conditions $f(0) = 1$ and $f(x \rightarrow \infty) = 0$,

$$f(x) = e^{-x/l}, \quad \text{with } l = (\lambda^{\alpha-1} d)^{1/\alpha}. \quad (13)$$

This exponential decrease of gas-phase molecular fraction f as a function of depth x into the cloud has an e -folding distance $l \propto \lambda^{1-1/\alpha}$, which, for $1 < \alpha < 2$ is shallower than the dependence on the mixing length λ obtained from the diffusion model (see equation 8). In Fig. 1, we show l versus λ for a cloud of density $n = 10^5 \text{ cm}^{-3}$ (giving $d = 10^{17} \text{ cm}$, from equation 4), for three different values of α .

From this figure, we see that, as α decreases, we obtain increasingly larger values of l for λ in the 10^{14} – 10^{17} cm range. In particular, for the example chosen in Section 2 (i.e. a cloud core with a characteristic size $L \sim 6 \times 10^{16} \text{ cm}$), if we choose a mixing length $\lambda \sim 0.01L \sim 6 \times 10^{14} \text{ cm}$ we can obtain an e -folding distance $l \sim 6 \times 10^{16} \text{ cm} \sim L$, when α is between 1.1 and 1.2. In Fig. 2, we show the characteristic penetration length l as a function of α for three values of the mixing length λ , where this fact can be seen. We note that, for $\lambda = 10^{15}$ the actual value of α for which $l \sim L$ is $\alpha = 1.12$. Therefore, if the mixing length λ , is to be kept small, as required by a turbulence model, the use of a non-local transport model with $\alpha \leq 1.12$ will be adequate in producing an overall transport that affects the whole volume of the cloud core.

One can note that in Fig. 1 there is a crossover point at $\lambda = d = 10^{17} \text{ cm}$, above which the behaviour is opposite to the one

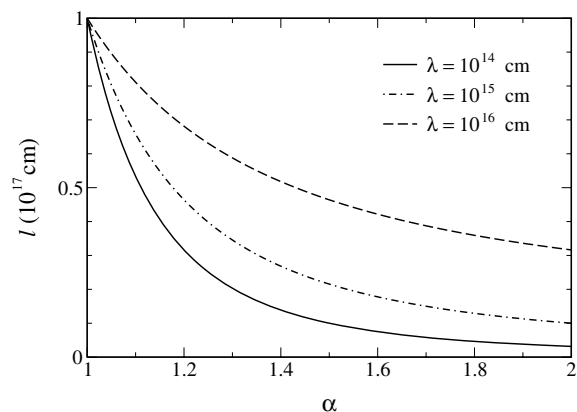


Figure 2. Transport penetration length as a function of the fractional parameter α for three values of the mixing length λ . For $\lambda = 10^{15}$, one obtains the required $l = 6 \times 10^{16}$ when $\alpha = 1.12$.

described before, in the sense that the fractional transport reduces the penetration length. This is due to the fact that for $\lambda > d$ the transport scale is dominated by the adsorption length. However, this region is not relevant to our model since in that case the mixing length is already larger than the cloud size and thus it does not represent a realistic turbulent state.

As mentioned above, the fractional diffusion model is physically related to a transport process in which the particles follow a random walk with non-Gaussian jump-size probability distribution functions. The parameter α is related to the distribution of jumps; for large steps the distribution has a power-law decay that goes as $\sim x^{-(\alpha+1)}$. In general the jump distribution is asymmetric, and in the extremal case it only exhibits algebraic decay in one direction. This is the situation for the model we took here, with only the right-fractional derivative. In this case, Levy flights have only a weak effect on transport, because the jump distribution does not have an algebraic tail for $x \rightarrow \infty$. Thus, a low value of α is needed in order to have an important contribution of the non-local transport. Strong non-locality involves Levy flights in the $x \rightarrow \infty$ direction. As discussed in the next section, this situation is captured by including the left-fractional derivative in the model.

4 TRANSPORT MODEL WITH STRONG NON-LOCALITY

It is important to mention that, in addition to the right-fractional derivative, one can use the *left* derivative defined as

$${}_a D_x^\alpha = \frac{1}{\Gamma(2-\alpha)} \frac{d^2}{dx^2} \int_a^x \frac{f(t) dt}{(x-t)^{\alpha-1}}, \quad 1 < \alpha < 2, \quad (14)$$

where a is an arbitrary constant. The most general transport model should in principle include both, the left and the right derivatives. These two operators have very different transport properties and including both, enriches the physics of the model considerably. In particular, as discussed in del-Castillo-Negrete et al. (2003), transport models with only a right (left) diffusion operator describe non-local transport caused by Levy flight to the left (right) of the domain. The model discussed in Section 3, assumes that a ‘microscopic’ level transport is caused by a random walk that is Gaussian to the right ($x \rightarrow \infty$) and Levy to the left ($x \rightarrow 0$). In this case, because of the boundary condition $f(0) = 1$, the Levy flights do not have an important effect. In particular, the solution exhibits an exponential decay similar to the one observed with regular diffusion, but with an enhanced diffusivity that leads to an increased penetration length. Intuitively, what is happening in this case is that the Levy flights are in a direction opposite to the ‘relevant’ transport direction. A similar situation was observed in del-Castillo-Negrete et al. (2003) where reaction–diffusion fronts propagating in a direction opposite to the direction of the Levy flights behave like the usual fronts but with an enhanced Kolmogorov speed.

Motivated by this discussion we consider here the fractional equation

$${}_0 D_x^\alpha f = \gamma f, \quad (15)$$

to describe a transport driven by Levy flights using the left-fractional derivative. Following del-Castillo-Negrete et al. (2003), we have defined the left spatial fractional derivative in the Caputo sense

$$\begin{aligned} {}_0 D_x^\alpha f &= {}_0 D_x^\alpha [f(x) - f(0) - f'(0)x] \\ &= \frac{1}{\Gamma(2-\alpha)} \int_0^x \frac{f''(t)}{(x-t)^{\alpha-1}} dt. \end{aligned} \quad (16)$$

for $1 < \alpha < 2$. Note that in del-Castillo-Negrete et al. (2003), the term $f'(0)x$ was not explicitly included because for a front problem it vanishes identically.

Using the Laplace transforms in space $\mathcal{L}f = \hat{f}(s) = \int_0^\infty e^{-sx} f(x) dx$, the solution of equation (15) in s -space is given by

$$\hat{f}(s) = \left(\frac{s^{\alpha-1}}{s^\alpha - \gamma} \right) f(0) + \left(\frac{s^{\alpha-2}}{s^\alpha - \gamma} \right) f'(0). \quad (17)$$

Introducing the Mittag–Leffler function (Podlubny 1999),

$$E_{\alpha\beta}(z) = \sum_{k=0}^{\infty} \frac{z^k}{\Gamma(\alpha k + \beta)}, \quad (18)$$

the inversion of the Laplace transform yields the solution

$$f(x) = f(0)E_{\alpha 1}(\gamma x^\alpha) + f'(0)x E_{\alpha 2}(\gamma x^\alpha). \quad (19)$$

In addition to the boundary condition at $x = 0$ the solution must satisfy the asymptotic condition $f \rightarrow 0$ as $x \rightarrow \infty$. The asymptotic behaviour of the Mittag–Leffler function, for $z > 0$

$$\begin{aligned} E_{\alpha\beta}(z) &= \frac{1}{\alpha} z^{(1-\beta)/\alpha} \exp(z^{1/\alpha}) - \sum_{k=0}^P \frac{z^{-k}}{\Gamma(\beta - \alpha k)} \\ &\quad + O(|z|^{-1-P}), \end{aligned} \quad (20)$$

contains exponentially growing and convergent terms. Using this, an analysis of the asymptotic behaviour of the solution in equation (19) implies that to kill the exponential growing terms the condition $f'(0) = -\gamma^{1/\alpha} f(0)$ must be imposed. This leads to the solution

$$f(x) = f(0) [E_{\alpha 1}(\gamma x^\alpha) - \gamma^{1/\alpha} x E_{\alpha 2}(\gamma x^\alpha)], \quad (21)$$

where $f(0) = 1$ is the boundary condition at $x = 0$ and as desired, $f(x \rightarrow \infty) = 0$.

From the definition of the Mittag–Leffler function in equation (18) it follows that $E_{21}(z^2) = \cos h(z)$ and $E_{22}(z^2) = (1/z) \sin h(z)$. Using this in equation (21) we recover, as expected, the solution of the regular fractional model in the $\alpha = 2$ case,

$$f(x) = [\cosh(\sqrt{\gamma}) - \sinh(\sqrt{\gamma})] = e^{-\sqrt{\gamma}x}. \quad (22)$$

The transport properties of the left-fractional transport model are very different from the properties of the right-fractional model and the standard diffusion model. In particular, compared with the other models, the left-fractional model is strongly non-local. The most striking manifestation of this strong non-locality is manifested in the algebraic decay of the transported grains far from $x = 0$. In particular, for $x \rightarrow \infty$ the leading term of the asymptotic expansion of equation (21) gives

$$f(x) \sim \frac{\gamma^{1-\alpha/\alpha}}{\Gamma(2-\alpha)} \frac{1}{x^{\alpha-1}}. \quad (23)$$

As shown in Figs 3 and 4, this algebraic decaying behaviour is to be contrasted with the exponential decay exhibited by the right-fractional model and the standard diffusive model.

To quantify the non-locality, and to compare with the other models, we define an *effective penetration length*, l_{eff} , by means of the relationship $f(x) = \exp(-x/l_{\text{eff}})$. (Clearly, $l_{\text{eff}} = l$ is constant for the previous two models.) For the Levy, left-fractional model, it follows from equation (21) that

$$l_{\text{eff}} = -x \left\{ \ln [E_{\alpha 1}(x^\alpha \gamma) - \gamma^{1/\alpha} x E_{\alpha 2}(x^\alpha \gamma)] \right\}^{-1}. \quad (24)$$

An expansion near $x = 0$ gives

$$l_{\text{eff}} = \gamma^{-1/\alpha} \left[1 + \frac{(\gamma^{1/\alpha} x)^\alpha}{\Gamma(\alpha + 1)} + \dots \right]. \quad (25)$$

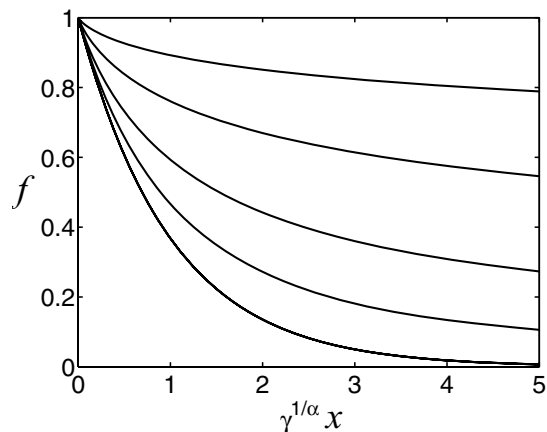


Figure 3. Concentration profile according to the solution in equation (21) of the left-fractional model in equation (15). The curve at the bottom gives the profile according to the local diffusive model ($\alpha \rightarrow 2$). The rest of the curves, from bottom to top, correspond to the 1.75, 1.5, 1.25 and 1.1 cases.

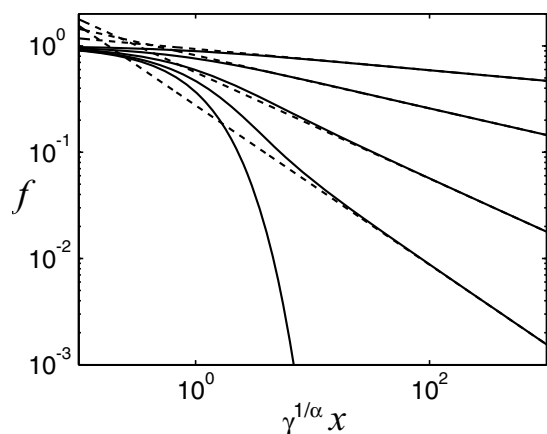


Figure 4. Same as Fig. 4, but in a log–log scale illustrating the algebraic decay of the concentration profile in the right-fractional model for large $\gamma^{1/\alpha} x$. The dashed lines correspond to the asymptotic analytical formula in equation (23).

As expected, in the $x \rightarrow 0$ limit we recover the weak non-local penetration length in equation (13) with $\gamma^{-1} = \lambda^{\alpha-1} d$. This verifies the intuition that the right-fractional model introduces weak, or ‘short-length’ non-locality. As observed in Fig. 5, due to the $x^{\alpha-1}$ scaling of the first-order correction, the convergence to the weak non-local result slows down as $\alpha \rightarrow 1$. On the opposite end, in the asymptotic $x \rightarrow \infty$ limit,

$$l_{\text{eff}} = x \left\{ \ln \left[\Gamma(2 - \alpha) (\gamma^{1/\alpha} x)^{\alpha-1} \right] \right\}^{-1}. \quad (26)$$

Fig. 5 illustrates the enhancement of the penetration length due to Levy flights in the $x \rightarrow \infty$ direction as predicted by the left-fractional model. This indicates that, as the cloud is penetrated, the influence of transport is dramatically increased, even for $\alpha \rightarrow 2$.

5 CONCLUSIONS

We have presented simple analytic considerations about the influence of turbulent transport on the chemistry of molecular clouds. We have considered a ‘toy model’ chemistry in which we have a single molecular species with a gas-phase abundance f (with $f =$

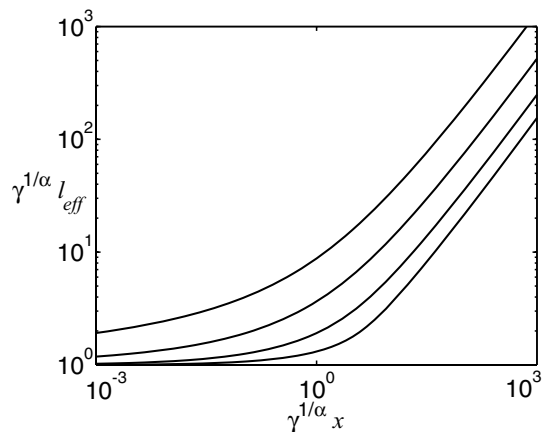


Figure 5. Effective penetration length in the left-fractional model of equation (15) according to equation (24). The different curves, from bottom to top, correspond to the $\alpha = 1.75, 1.5, 1.25$ and 1.1 cases. By definition, the $\alpha \rightarrow 2$ diffusive limit corresponds to the horizontal line $\gamma^{1/\alpha} l_{\text{eff}} = 1$.

1 at the surface of the homogeneous, slab cloud), and a rate R of adsorption on to grains.

If we introduce this idealized chemistry into a turbulent diffusion model, we find that f falls exponentially with distance into the cloud, with an e -folding length which depends on the adsorption rate and on the mixing length λ (see equation 4). We find that for the case of a dense cloud core, in order for the turbulent diffusion to have an important effect on the general structure of the cloud chemistry, we need to have λ comparable to the size of the cloud.

We have then described two non-local turbulent transport models based on partial spatial derivatives of the order of $1 < \alpha < 2$, which have been used for modelling the role of Levy-flights in reaction–diffusion systems (del-Castillo-Negrete et al. 2003) and anomalous turbulent transport in magnetically confined plasmas (del-Castillo-Negrete et al. 2004, 2005). For our ‘toy model’ chemistry, the first of the models also leads to an exponential decay of the gas-phase molecular fraction f as a function of distance into the cloud. However, with an $\alpha = 1.25$ value, we find that for mixing lengths $\lambda \sim 0.01L$ (where L is the characteristic size of the cloud) we already obtain penetration lengths $l \sim L$ (see equation 13 and Fig. 1). Therefore, this non-local transport model produces substantial effects on the cloud chemistry for mixing length values which are probably more representative of the sizes of the eddies which form the turbulent structures of molecular clouds. For the second non-local model, the dominance of large Levy flights produces a striking effect on the penetration length, making it very large, even for small mixing lengths, for any value of α between 1 and 2. Our results, then would indicate that the non-local transport in molecular clouds might be dominated by internal structures that link quite distant regions.

These encouraging results appear to justify applying the non-local transport models described in Sections 3 and 4 to a much more complex chemical network including several species and many reactions. However, the semi-empirical nature of this model (a characteristic shared by turbulent diffusion models) will eventually require a calibration of the model parameters (namely, the order α of the derivatives and the mixing length λ , see equations 9 and 10). Such a calibration could be carried out either by comparisons with observations of real molecular clouds (which is of course a far from simple proposition) or by comparing the predictions from this model with numerical simulations which include both the 3D MHD and

the chemical evolution. As such simulations are not yet available, this second possibility is also not straightforward.

ACKNOWLEDGMENTS

This work was supported by the CONACyT grants 36572-E, 41320, 43103-F and 44324-F and the DGAPA (UNAM) grants IN 112602, IN 113605 and IN 115205. DCN acknowledges support from the Oak Ridge National Laboratory, managed by UT-Battelle, LLC, for the US Department of Energy under contract Grant No. DE-AC05-00OR22725.

REFERENCES

- Boland W., de Jong T., 1982, *ApJ*, 261, 110
 Cantó J., Raga A. C., 1991, *ApJ*, 372, 646
 Charnley S. B., Dyson J. E., Hartquist T. W., Williams D. A., 1988a, *MNRAS*, 231, 269
 Charnley S. B., Dyson J. E., Hartquist T. W., Williams D. A., 1988b, *MNRAS*, 235, 1257
 Chièze J. P., Pineau des Forêts G., 1989, *A&A*, 221, 89
 Chièze J. P., Pineau des Forêts G., Herbst E., 1991, *ApJ*, 373, 110
 del-Castillo-Negrete D., Carreras B. A., Lynch V. E., 2003, *Phys. Rev. Lett.*, 91, 018302
 del-Castillo-Negrete D., Carreras B. A., Lynch V. E., 2004, *Phys. Plasmas*, 11, 3854
 del-Castillo-Negrete D., Carreras B. A., Lynch V. E., 2005, *Phys. Rev. Lett.*, 94, 065003
 Garrod R. T., Williams D. A., Hartquist T. W., Rawlings J. M. C., Viti S., 2005, *MNRAS*, 356, 654
 Garrod R. T., Williams D. A., Rawlings J. M. C., 2006, *ApJ*, 638, 827
 Iglesias E., 1977, *ApJ*, 218, 697
 Leger A., Jura M., Omont A., 1985, *A&A*, 144, 147
 Metzler R., Klafter J., 2000, *Phys. Rep.*, 339, 1
 Morata O., Girart J. M., Estalella R., 2003, *A&A*, 435, 113
 Morata O., Girart J. M., Estalella R., 2005, *A&A*, 397, 181
 Nejad L. A. M., Williams D. A., Charnley S. B., 1990, *MNRAS*, 246, 183
 Norman C., Silk J., 1980, *ApJ*, 238, 138
 Podlubny I., 1999, *Fractional Differential Equations*. Academic Press, San Diego
 Rawlings J. M. C., Hartquist T. W., 1997, *ApJ*, 487, 67
 Rawlings J. M. C., Hartquist T. W., Menten K. M., Williams D. A., 1992, *MNRAS*, 255, 471
 Redman M. P., Rawlings J. M. C., Nutter D. J., Ward-Thompson D., Williams D. A., 2002, *MNRAS*, 337, L17
 Steinacker J., Bacmann A., Henning Th., Klessen R., Stickelel M., 2005, *A&A*, 434, 167
 Viti S., Natarajan S., Williams D. A., 2002, *MNRAS*, 336, 797
 Whittet D. C. B., 2002, *Dust in the Galactic Environment*, 2nd edn. Institute of Physics, Bristol
 Willacy K., Williams D. A., 1993, *MNRAS*, 260, 635
 Williams D. A., 2003, in Pirronello V., ed., *Solid State Astrochemistry*. Kluwer Academic Publishers, Dordrecht, p. 1
 Williams D. A., Hartquist T. W., 1984, *MNRAS*, 210, 141
 Xie T., Allen M., Langer W. D., 1995, *ApJ*, 440, 674

This paper has been typeset from a $\text{\TeX}/\text{\LaTeX}$ file prepared by the author.